

A Quality Diversity Approach to Automatically Generating Human-Robot Interaction Scenarios in Shared Autonomy

Matthew Fontaine and Stefanos Nikolaidis

Abstract

As interactions between humans and robots grow in scale and complexity, the human-robot interaction (HRI) research community needs new computational methods to automatically evaluate the performance of novel algorithms and applications. Strong evaluation methods should reduce researcher bias and explore the diverse scenarios of interaction between humans and robots. We propose quality diversity (QD) algorithms as a method for simultaneously exploring both environments and human actions to discover diverse failure scenarios. We focus on the shared autonomy domain, where the robot attempts to infer the goal of a human operator. We evaluate our approach by automatically generating scenarios for two published algorithms in this domain: shared autonomy via hindsight optimization and linear policy blending. Some of the generated scenarios confirm previous theoretical findings, while others are surprising and bring about a new understanding of state-of-the-art implementations. Our experiments show that QD outperforms Monte-Carlo simulation and optimization based methods in effectively searching the scenario space, highlighting its promise for automatic evaluation of algorithms in shared autonomy.

1 Introduction

We present a method for automatically generating human-robot interaction (HRI) scenarios in shared autonomy. To understand the importance of this problem, consider how human-robot interaction algorithms, that is algorithms that enable deployed robotic systems to operate with and around people, are currently developed and tested. First, new algorithms are developed by researchers to solve a specific HRI problem. Next, the researchers *themselves* hand-author a small number of specific scenarios to evaluate their algorithm. Finally, good algorithms are implemented in industry and evaluated via Monte-Carlo simulation or hand-authored tests. We aim to improve the second and third stages of this process.

Consider as an example a manipulation task, where the robot runs a shared autonomy algorithm [35]. A user provides inputs to a robotic manipulator through a joystick, guiding the robot towards a desired goal, e.g., grasping a bottle on the table. The robot does not know the goal of the user in advance, but infers their desired goal in real-time by observing their inputs and assisting them by moving autonomously towards that goal. Performance of the algorithm is assessed by how fast the robot reaches the goal. However, different environments and human behaviors could cause the robot to fail, by picking the wrong object or colliding with obstacles.

How should HRI researchers evaluate this algorithm? Typically, such algorithms are evaluated with human subject experiments [64].

Matthew Fontaine and Stefanos Nikolaidis are with the Department of Computer Science, University of Southern California, Los Angeles, USA {mfontain, nikolaid}@usc.edu .

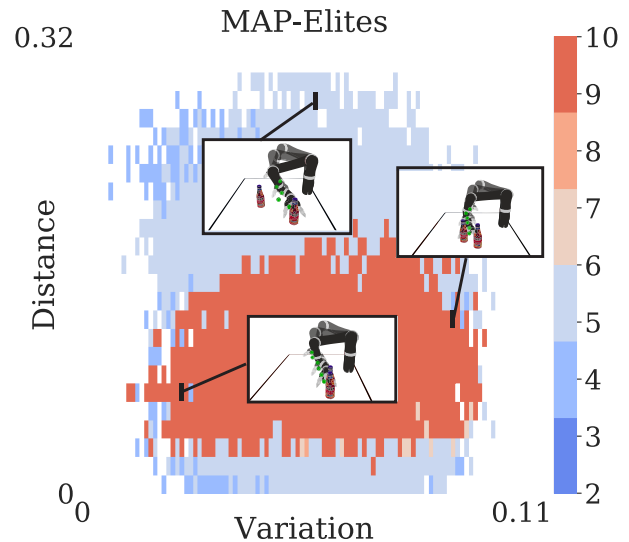


Figure 1: An example archive of solutions returned by the quality diversity algorithm MAP-Elites. The solutions in red indicate scenarios where the robot fails to reach the desired user goal in a simulated shared autonomy manipulation task. The scenarios vary with the environment (y-axis: distance between the two candidate goals) and human inputs (x-axis: variation from optimal path).

The researchers themselves typically hand-author the evaluation scenarios, which in our example is bottle locations and subject instructions. As the researchers created the new algorithm, they may unconsciously place bottles far apart or request participants to interact in a specific way. The design choices of the hand-authored scenarios may be biased in a way that do not fully illustrate how the algorithm performs in general.

Another approach is simulating agent behaviors by randomly sampling from models of human behavior and interaction protocols (e.g., [5, 63]). However, exploring the continuous, high-dimensional space of all possible environments and human action sequences is infeasible. At the same time, our focus is often not how an HRI algorithm performs on any environment or human action sequence. Our questions are much more specific, e.g., how irrational can the human be before the algorithm breaks? Or, in the aforementioned example task, how far apart do two candidate goals have to be for the robot to disambiguate the human intent?

Our key insight is that quality diversity (QD) algorithms [56] – population-based stochastic algorithms designed to generate a diverse collection of high-quality solutions – can effectively explore

a wide spectrum of human and robot behaviors when evaluating HRI algorithms and discover diverse failure cases. We propose QD as a scenario generation method for automatically discovering limiting cases to compare the performance of HRI algorithms in a shared autonomy domain, where a robotic manipulator attempts to infer the user’s goal based on their inputs.

We show that the QD algorithm MAP-Elites [13, 51] outperforms standard Monte Carlo simulation (random search) and CMA-ES [27], a state-of-the-art derivative-free optimization algorithm, in finding failure scenarios for the “shared autonomy with hindsight optimization” [36], a powerful and widely used algorithm, by searching a continuous scenario space of environments and human actions.

We reproduce some of the failure scenarios automatically discovered in simulation on a real robot with human inputs. While some scenarios are expected, e.g., the robot approaches the wrong goal if the human provides very noisy inputs, others are surprising, e.g., the robot never reaches the desired goal even for a nearly optimal user if the two objects are aligned in column formation in front of the robot (Fig. 1)!

QD algorithms treat the algorithm being tested as a “black box”, without any knowledge of its implementation, which makes them applicable to multiple domains. Overall, we are excited that QD can bring about a new understanding of the strengths and limitations of current and future HRI algorithms, opening up a great number of scientific challenges and opportunities to which we look forward.

2 Background

Automatic Scenario Generation Automatically generating scenarios is a long standing problem in human training [31], with the core challenge being the generation of *realistic* scenarios [49]. Previous work [71] has shown that optimization methods can be applied to generate scenarios by maximizing a scenario quality metric. Scenario generation has been applied extensively to evaluating autonomous vehicles [2, 6, 22, 53, 60].

Automatic scenario generation is closely related to the problem of generating video game levels in procedural content generation (PCG) [29, 61]. An approach gaining popularity is procedural content generation through quality diversity (PCG-QD) [25], which leverages QD algorithms to drive the search for interesting and diverse content.

Quality Diversity and MAP-Elites. QD algorithms differ from pure optimization methods, in that they do not attempt to find a single optimal solution, but a collection of good solutions that differ across specified dimensions of interest. For example, QD algorithms have generated video game levels of varying number of enemies or tile distributions [20, 38], and objects of varying shape complexity and grasp difficulty [50].

MAP-Elites [13, 51] is a popular QD algorithm that searches along a set of explicitly defined attributes called *behavior characteristics* (BCs), which induce a Cartesian space called a *behavior space*. The behavior space is tessellated into uniformly spaced grid cells. In each cell, the algorithm maintains the highest performing solution, which is called as *elite*. The collection of elites returned by the algorithm forms an *archive* of solutions.

MAP-Elites populates the archive by first randomly sampling a population of solutions, and then selecting the elites – which are

the top performing solutions in each cell of the behavior space – at random and perturbing them with small variations. The objective of the algorithm is two-fold: maximize the number of filled cells (coverage) and maximize the quality of the elite in each cell. Recent algorithms have focused on how the behavior space is tessellated [19, 62], as well as how the each elite is perturbed [66].

Coverage-Driven Testing in HRI. Previous work [4, 5] explored test generation in human-robot interaction using Coverage-Driven Verification (CDV), emulating techniques used in functional verification of hardware designs. Human action sequences were randomly generated in advance and with a model-based generator which modeled the interaction with Probabilistic-Timed Automata. Instead, we focus on online scenario generation by searching over a set of scenario parameters; the generator itself is agnostic to the underlying HRI algorithm and human model. Previous work [3] has also used Q-learning to generate plans for an agent in order to maximize coverage. Our focus is both on coverage and quality of generating scenarios, with respect to a prespecified set of behavioral characteristics that we want to cover. In contrast to previous studies that simulate human actions, *we jointly search for environments and human/agent behaviors*.

Shared Autonomy. Shared autonomy (also: shared control, assistive teleoperation) combines human teleoperation of a robot with intelligent robotic assistance. It has been applied in the control of robotic arms [16, 24, 30, 33, 35, 37, 47, 52, 55], the flight of UAVs [23, 43, 58], and robot-assisted surgery [44, 59]. It has been used with a variety of interfaces, such as whole body motions [16], natural language [15], laser pointers [67], brain-computer interfaces [52], body-machine interfaces [34] and eye gaze [10, 35]. Shared autonomy first predicts the human’s goal, often through machine learning methods trained from human demonstrations [28, 40, 69], or through maximum entropy inverse optimal control [70]. Second, shared autonomy provides assistance, which often involves blending the user’s input with the robot assistance to achieve the predicted goal [16, 17, 39]. Assistance can also provide task-dependent guidance [1], manipulation of objects [37], or mode switches [30].

Shared Autonomy via Hindsight Optimization In shared autonomy via hindsight optimization [36] assistance blends user input and robot control based on the confidence of the robot’s goal prediction. The problem is formulated as a Partially Observable Markov Decision Process (POMDP), wherein the user’s goal is a latent variable. The system models the user as an approximately optimal stochastic controller, which provides inputs so that the robot reaches the goal as fast as possible. The system uses the user’s inputs as observations to update a distribution over the user’s goal, and assists the user by minimizing the expected cost to go – estimated using the distance to goal – for that distribution. Since solving a POMDP exactly is intractable, the system uses the hindsight optimization (QM DP) approximation [46]. The system was shown to achieve significant improvements in efficiency of manipulation tasks in an object-grasping task [36] and more recently in a feeding task [35]. We refer to this algorithm simply as *hindsight optimization*.

3 Problem Statement

Given a robotic system interacting with a human, the goal is to generate scenarios that make the system perform poorly, while

ensuring the generated scenarios cover a range of prespecified dimensions of interest.

Let R be a single robot interacting with a single human H. The human takes continuous actions $u_H \in \mathbb{R}^{m^H}$ where m^H is the dimensionality of the human actions, following a deterministic human policy $\pi_H(x_H, x_W, \theta)$, where x_W is the world (and robot) state, x_H is the internal state of the human, and $\theta \in \mathbb{R}^{n_\theta}$ is a set of policy parameters. The robot observes x_W and the human action u_H and takes an action $u_R = \pi_R(x_W, u_H)$. The state of the world and the human change deterministically with dynamics: $\dot{x}_W = g_W(x_W, u_R, u_H)$, $\dot{x}_H = g_H(x_W, x_H, u_R)$. H and R act in the world for a time horizon T , or until they reach a final state $x_f \in X_R$.

A *scenario* consists of the parameters θ of the human policy π_H , and a set of parameters $\phi \in \mathbb{R}^{n_\phi}$, which parameterize the initial world x_W^0 and human x_H^0 states. To evaluate a scenario, we assume a function $f(x_W^{0..T}, x_H^{0..T}) \rightarrow \mathbb{R}$ that maps the state history to a real-number. We call this an *assessment* function, which measures the performance of the robotic system R. We also assume M user-defined functions, $b_i(x_W^{0..T}, x_H^{0..T}) \rightarrow \mathbb{R}$, $i \in [M]$. These functions measure aspects of generated scenarios that should vary (i.e. human rationality). We call these functions *behavioral characteristics* (BCs), which induce a Cartesian space called a *behavior space*.

Given the deterministic dynamics, we can directly map a value assignment of the parameters (θ, ϕ) to a state history $(x_W^{0..T}, x_H^{0..T})$ and therefore to an assessment $f(\theta, \phi)$ and a set of BCs $b(\theta, \phi)$. We assume that the behavior space is partitioned into N cells, which form an *archive* of scenarios, and we let (θ_i, ϕ_i) be the parameters of the scenario occupying cell $i \in [N]$.

The objective of our scenario generator is to fill in as many cells of the archive as possible with scenarios of high assessment f :

$$M(\theta_1, \phi_1, \dots, \theta_N, \phi_N) = \max \sum_{i=1}^N f(\theta_i, \phi_i) \quad (1)$$

Shared Autonomy. A special case of this setting is the shared autonomy domain. In shared autonomy, the human state is specified by a desired goal $x_H \equiv g_H \in G$ among a set of candidate goals G , known to the robot. The user does not change their intended goal throughout the task, so that $\dot{x}_H = 0$. The human actions are inputs to the system, e.g., through a joystick interface, while only the robot actions affect the physical state of the world, i.e., $\dot{x}_W = g_W(x_W, u_R)$.

4 Finding Failure Scenarios

The hindsight optimization algorithm [36] achieved significant benefits, compared to previous blending approaches [16], when measuring task efficiency in grasping scenarios. To evaluate the method, the authors conducted a human subjects experiment, where subjects attempted to reach one out of three candidate goal objects placed one next to each other in a line in front of the robot.

We wish to generate scenarios that show the limits of the system: how noisy can the human be without the system failing to reach the desired goal? How does distance between candidate goals affect the system's performance? Intuitively, noisier human inputs and smaller distances between goals would make the inference of the user's goal harder and thus make the system more likely to fail.

These dimensions of interest are the behavioral characteristics (BC) b : attributes that we wish to obtain coverage for. For each BC

value assignment, we will search for the hardest possible scenario, that is the scenario that has the highest assessment function f , as specified in Sec. 3, where higher assessment results in worst performance of the hindsight optimization algorithm.

4.1 Experimental Design

We evaluate our scenario generation system on the publicly available implementation of the hindsight optimization algorithm [42], which runs on the OpenRAVE [14] simulation environment. Experiments were conducted with a Gen2 Jaco2 Lightweight manipulator. For each goal object we assume one target grasp location, on the side of the object that is facing the robot.

We evaluate the hindsight optimization algorithm by generating *scenarios*, where each scenario consists of an environment and a parameterized trajectory of user inputs. We then execute the hindsight optimization algorithm until the end-effector reaches the user's goal, or when the maximum time (10 s) has elapsed.

4.2 Scenario Parameters

Following the specification of Sec. 3, we define the scenario parameters (θ, ϕ) that induce both the human policy and environment.

Goal Objects: We simulate an environment with a set of n goal objects placed on a table, so that $\phi = (g^1, \dots, g^n)$. We specified the range of the coordinates $g_x \in [0, 0.25]$ (in meters), $g_y \in [0, 0.2]$ so that the goals are always reachable by the robot's end-effector. Similarly to previous work [36], the robot is positioned so as to face the objects (Fig. 4). However, rather than assuming that all objects are aligned horizontally facing the robot, each object can be placed anywhere within the given range.

Human Inputs: Previous work assumes that the user attempts to reach the desired goal as efficiently as possible, without modeling the robot's actions [36]. Our pilot studies have also shown that user inputs are typically not of constant magnitude. Instead, inputs spike when users wish to "correct" the robot's path, and decrease in magnitude afterwards when the robot takes over.

Following these assumptions, we model the user by specifying a set of equidistant waypoints in Cartesian space forming a straight line that starts from the initial position of the robot's end-effector and ends at the desired goal of the user. At each timestep, we model the user as providing a translational velocity command u_H for the robot's end-effector towards the next waypoint, proportional to the distance to that waypoint.

We then allow for noise in the input by adding a disturbance $d \in [-0.05, 0.05]$ for each of the intermediate waypoints in the x -axis (Fig. 4). We selected $m = 5$ intermediate waypoints, so that $\theta = (d_1, \dots, d_5)$.

Assessment function: We use as an assessment function f in Eq. 1 the time to reach the user's goal. If the robot does not reach the user's goal by the maximum time (10s), the task terminates.

In total, the search parameters include the 2D position of n goals on the table and the 1D disturbances of m intermediate waypoints, resulting in a $2n + m$ -dimensional continuous search space.

4.3 Behavioral Characteristics

Distance Between Goals: How far apart the human goal is from other candidate goals in a scenario plays an important role in disambiguating the human intent. The reason is that the hindsight optimization implementation models the human user as minimizing a cost function proportional to the distance between the robot and the desired goal. The framework then infers the user's goal by using the user inputs as observations; the more unambiguous the user input, the more accurate the inference of the system. Therefore, we expect that the further away the human goal g_H is from the nearest goal g_N , the better the system will perform. We define this BC as:

$$BC_1 = \|g_H - g_N\|_2 \quad (2)$$

Given the range of the goal coordinates, the range of this BC is $[0, 0.32]$. In practice, there will be always a minimum distance between two goal objects because of collisions, but this does not affect our search, since we can ignore cases where the objects collide. We partitioned this behavior space to 25 uniformly spaced intervals.

Human Variation: We expect noise in the human inputs to affect the robot's inference of the user's goal and thus the system's performance. We capture variation from the optimal path using the root sum of the squares of the disturbances d_i applied to the m intermediate waypoints.

$$BC_2 = \sqrt{\sum_{i=1}^m d_i^2} \quad (3)$$

A value of 0 indicates a straight line to the goal. Since we have $d_i \in [-0.05, 0.05]$ (Sec. 4.2), the range of this BC is $[0, 0.11]$. We partitioned this behavior space to 100 uniformly spaced intervals.

Human Rationality: If we model the user as a noisily rational decision maker [8, 18], we can interpret deviations from the optimal trajectory of human inputs as a result of how "rational" or "irrational" the user is. Formally, we let x_R be the 3D position of the robot's end-effector and u_H be the velocity controlled by the user in Cartesian space. We model the user as following Boltzmann policy $\pi_H \mapsto P(u_H | x_R, g_H, \beta)$, where β is the rationality coefficient – also interpreted as the expertise [37] – of the user and Q_{g_H} is the value function from x_R to the goal g_H .

$$P(u_H | x_R, g_H, \beta) \propto e^{-\beta Q_{g_H}(x_R, u_H)} \quad (4)$$

Let $Q_{g_H} = -\|u_H\|_2 - \|x_R + u_H - g_H\|_2$ [18], so that the user minimizes the distance to the goal. Observe that if $\beta \rightarrow \infty$, the human is rational, providing velocities exactly in the direction to the goal. If $\beta \rightarrow 0$, the human is random, choosing actions uniformly.

We can estimate the user's rationality, given their inputs, with Bayesian inference [18]:

$$P(\beta | x_R, g_H, u_H) \propto P(u_H | x_R, g_H, \beta) P(\beta) \quad (5)$$

Since the human inputs change at each waypoint (Section 4.2), we perform $m + 1$ updates, at the starting position and at each intermediate waypoint, on a finite set of discrete values β . Following previous work [37], we set the rationality range $\beta \in [0, 1000]$. We then choose as behavioral characteristic the value with the maximum a posteriori probability at the end of the task:

$$BC3 = \operatorname{argmax} P(\beta | x_R^{0..T}, g_H, u_H^{0..T}) \quad (6)$$

We partitioned the space to 101 uniformly spaced intervals.

4.4 Independent Variables

The experiment has two independent variables, the *behavior space* and the *search algorithm*.

Behavior Space: (1) Distance between $n = 2$ goal objects (BC1) and human rationality (BC3), (2) Distance between $n = 2$ goal objects (BC1) and human variation (BC2), and (3) Distance between human goal and nearest goal for $n = 3$ goals (BC1) and human variation (BC3).

Search Algorithm: We evaluate three different search methods: MAP-Elites, CMA-ES and random search. The Covariance Matrix Adaptation Evolution Strategy (CMA-ES) is one of the most competitive derivative-free optimizers for single-objective optimization of continuous spaces (see [26, 27]). In random search we use Monte Carlo simulation where scenario parameters are sampled uniformly within their prespecified ranges. We implemented a multi-processing system on an AMD Ryzen Threadripper 64-core (128 threads) processor, as a master search node and multiple worker nodes running separate OpenRAVE processes in parallel, which enables simultaneous evaluation of many scenarios. Random search and MAP-Elites run asynchronously on the master search node, while CMA-ES synchronizes before each covariance matrix update. We generated 10,000 scenarios per trial, and ran 45 trials, 5 for each algorithm and behavior space. One trial parallelized into 100 threads lasted approximately 20 minutes.

4.5 Algorithm Tuning

MAP-Elites first samples uniformly the space of scenario parameters θ, ϕ within their prespecified ranges (Sec. 4.2) for an initial population of 100 scenarios. The algorithm then randomly perturbs the elites (scenarios from the archive) with Gaussian noise scaled by a σ parameter. The two scenario parameters, position of goal objects ϕ and human waypoints θ , are on different scales, thus we specified different σ for each: $\sigma_\phi = 0.01, \sigma_\theta = 0.005$.

To generate the scenarios for random search, we uniformly sample scenario parameters within their prespecified ranges, a method identical to generating the initial population of MAP-Elites.

For CMA-ES, we selected a population of $\lambda = 12$ following the recommended setting from [27]. To encourage exploration, we used the bi-population variant of CMA-ES with restart rules [7, 26], where the population doubles after each restart, and we selected a large step size, $\sigma = 0.05$. Since the two search parameters are in different scales, we initialized the diagonal elements of the covariance matrix C , so that $c_{ii} = 1.0, i \in [2n]$ and $c_{ii} = 0.5, i \in \{2n + 1, \dots, 2n + m\}$, with $2n$ and m the dimensionality of the goal object and human input parameter spaces respectively.

Both CMA-ES and MAP-Elites may sample scenario parameters that do not fall inside their prespecified ranges. Following recent empirical results on bound constraint handling [9], we adopted a resampling strategy, where new scenarios are resampled until they fall within the prespecified range.

4.6 Measures

We wish to measure both the diversity and the quality of scenarios returned by each algorithm. These are combined by the QD-Score

	BC1 & BC3, 2 goals		BC1 & BC2, 2 goals		BC1 & BC2, 3 goals	
Algorithm	Coverage	QD-Score	Coverage	QD-Score	Coverage	QD-score
Random	22.3%	3464	48.4%	7782	41.9%	7586
CMA-ES	24.8%	4540	38.9%	7422	34.5%	7265
MAP-Elites	62.8%	10128	63.0%	11216	57.4%	11204

Table 1: Results: Percentage of cells covered (coverage) and QD-Score after 10,000 evaluations, averaged over 5 trials.

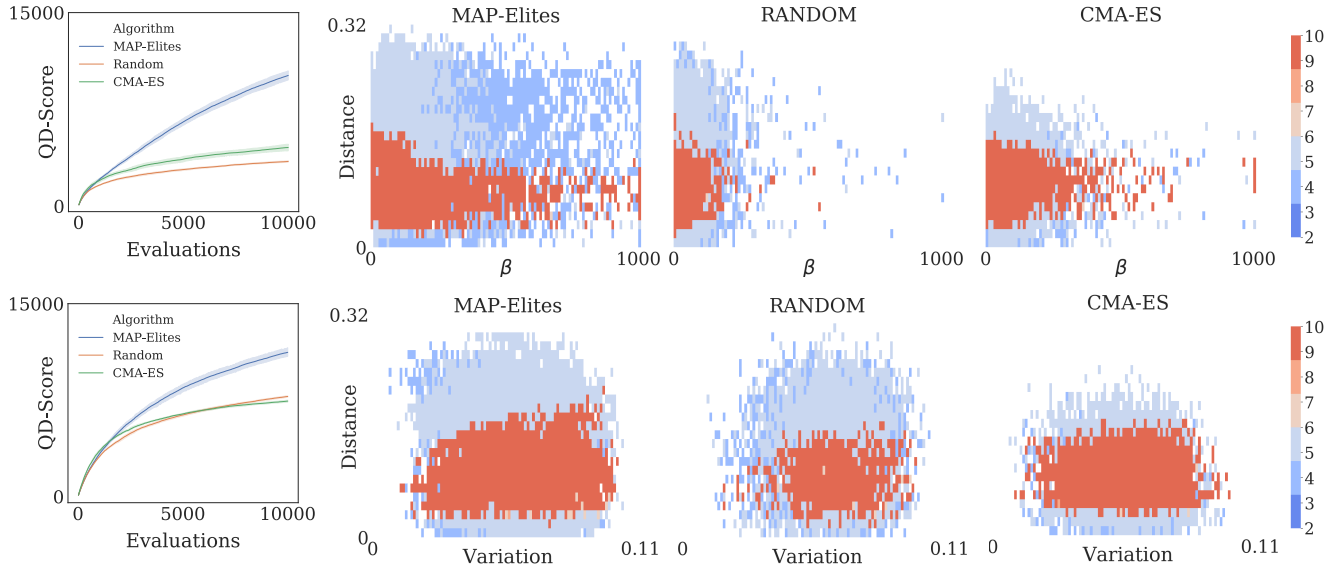


Figure 2: QD-Scores over evaluations (generated scenarios) and example archives returned by the three algorithms for the first two behavior spaces of Table 1. The colors of the cells in the archives represent time to task completion in seconds.

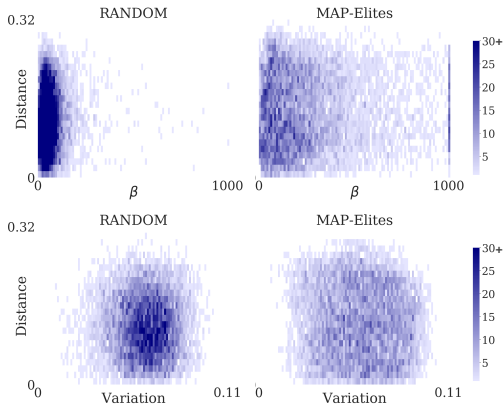


Figure 3: Distribution of cells explored for random search and MAP-Elites. The cell colors represent frequency counts.

metric [57], which is defined as the sum of f values of all elites in the archive (Eq. 1 in Sec. 3). Similarly to previous work [21], we

compute the QD-Score of CMA-ES and random search for comparison purposes by calculating the behavioral characteristics for each scenario and populating a pseudo-archive. As an additional metric of diversity we compute the coverage, that is the number of occupied cells in the archive divided by the total number of cells.

4.7 Hypothesis

We hypothesize that MAP-Elites will result in larger QD-Score and coverage than both CMA-ES and random search.

Previous work [19, 21] has shown that behavior spaces are typically distorted: uniformly sampling the search parameter space results in samples concentrated in small areas of the behavior space. Therefore, we expect random search to have small coverage of the behavior space. Additionally, since random search ignores the assessment function f , we expect the quality of the found scenarios in the archive to be low.

CMA-ES moves with a single large population that has global optimization properties. Therefore, we expect it to concentrate in regions of high-quality scenarios, rather than explore the archive. On the other hand, MAP-Elites both expands the archive and maximizes the quality of the scenarios within each cell.

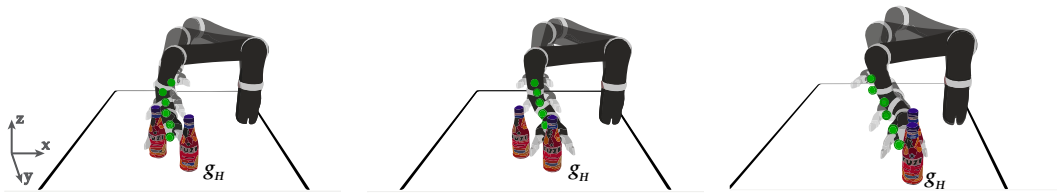


Figure 4: (Left) The robot fails to reach the user’s goal g_H because of the large deviation in human inputs from the optimal path. The waypoints of the human inputs are indicated with green color. **(Center)** We show for comparison how the robot would act if human deviation was 0 (optimal human). **(Right)** The robot fails to reach the user’s goal g_H (bottle furthest away from the robot), even though the human provides a near optimal input trajectory.

4.8 Analysis

Table 1 summarizes the performance of the three algorithms, for each of the three behavior spaces. We conducted a two-way ANOVA to examine the effect of the behavior space and the search algorithm on the QD-Score and coverage. There was a statistically significant interaction between the search algorithm and the behavior space for both QD-Score ($F(4, 36) = 62.39, p < 0.001$) and coverage ($F(4, 36) = 77.92, p < 0.001$). Simple main effects analysis with Bonferroni correction showed that MAP-Elites outperformed CMA-ES and random search in both QD-Score and coverage ($p < 0.001$ in all comparisons). This result supports our hypothesis.

Fig. 2 shows the improvement in the QD-Score over time and one example archive from each algorithm for the first two behavior spaces. MAP-Elites visibly finds more cells and of higher quality (red color), illustrating its ability to cover larger areas of the archive with high-quality scenarios. As expected, CMA-ES concentrates in regions of high-quality scenarios but has small coverage.

Random search covers a smaller area of the map, compared to MAP-Elites, because of the behavior space *distortion*, shown in Fig. 3. Even though the search parameters are sampled uniformly, scenarios are concentrated on the left side of the archive specified by the human rationality and distance between goals BCs (Fig. 3-top). This occurs because if any of the sampled waypoints deviates from the optimal path, low values of rationality become more likely. In the human variation and distance between goals BCs, the distribution of scenarios generated by random search is concentrated in a small region near the center (Fig. 3-bottom). This is expected, since the two BCs are Euclidean norms of random vectors (see [68]). On the other hand, MAP-Elites selects elite scenarios from the archive and perturbs them with Gaussian noise, instead of uniformly sampling the scenario parameters, resulting in larger coverage.

4.9 Interpreting the Archives

In the generated archives (Fig. 2), each cell contains an elite, which is the scenario that achieved the maximum assessment value (time to complete the task) for that cell. We can therefore replay the elites in different regions of the archives to explain the system’s performance. We focus on the first two behavior spaces using the archives generated with MAP-Elites in Fig. 2, since the MAP-Elites archives had the largest QD-Score and coverage.

We observe that if the distance between goals is large and the human is nearly optimal, the robot performs the task efficiently.

This is shown by the blue color in the top-right of the first behavior space (distance and human rationality β). We observe the same for large distance and small variation in the second behavior space.

We then explore different types of scenarios where the robot fails to reach the user’s goal by the maximum time (10s), indicated by the red cells in the archives. When human variation is large (or equivalently rationality is low), the human may provide inputs that guide the robot towards the wrong goal. Since the robot updates a probability distribution over goals based on the user’s input [36] and the robot assumes that the user minimizes their distance to their desired goal, noisy inputs may result in assigning a higher probability to the wrong goal and the robot will move towards that goal instead. Fig. 4(left) shows the execution trace of one elite where this occurs. Fig. 1 shows the position of this elite in the archive. Fig. 4(center) shows how the robot would reach the desired goal if the human had behaved optimally, instead.

What is surprising, however, is that the robot does not reach the user’s goal even in parts of the behavior space where human variation is nearly 0 (or equivalently rationality is very high), that is when the human provides a nearly optimal input trajectory! Fig. 4(right) reveals a case, where the two goal objects are aligned one closely behind the other. The robot approaches the first object, on the way towards the second object, and stops there.

What is interesting in both scenarios is that the robot gets “stuck” at the wrong goal, even when the simulated user continues providing inputs to their desired goal! Inspection of the publicly available implementation [42] of the algorithm shows that this results from the combination of two factors: the robot’s cost function and the human inputs.

Cost Function. The cost function that the robot minimizes is specified as a constant cost when the robot is far away from the goal and as a smaller linear cost when the robot is near the target [35] (distance to target is smaller than a threshold). This makes the cost of the goal object near the robot significantly lower than the cost of the other goal objects, which results in the probability mass of the goal prediction to concentrate on that goal. While this can help the user align the end-effector with the object (see [35]), it can also lead to incorrect inference, if the robot approaches the wrong goal on its way towards the correct goal or because of noisy human input. We confirmed that removing the linear term from the cost function results in the robot reaching the right goal in both examples.

Human Inputs. The hindsight optimization implementation minimizes a cost function specified as the sum of two quadratic terms, the expected cost-to-go to assist for a distribution over goals, and a term penalizing disagreement with the user’s input. The first-order approximation of the value function leads to an interpretation of the final robot action $u_R = u_R^A + u_R^U$ as the sum of two independent velocity commands, an “autonomous” action u_R^A towards the distribution over goals and an action that follows the user input u_R^U , as if the user was directly teleoperating the robot (see [35]).

We have simulated the human inputs, so that they provide a translational velocity command towards the next waypoint, proportional to the distance of the robot’s end-effector to that waypoint (Sec. 4.2). This results in a term u_R^U of small magnitude when the end-effector is close to one of the waypoints. If at the same time the robot has high confidence on one of the goals, u_R^A will point in the direction of that goal and it will cancel out any term u_R^U that attempts to move the robot in the opposite direction.

We confirmed that, if the user instead applied the maximum possible input towards their desired goal, the robot would get “unstuck,” so a real user would always be able to eventually reach their desired goal. However, this requires effort from the user who would need to “fight” the robot. We show this in the supplemental video.¹

Overall, the archive reveals limitations that depend on *how the goal objects are aligned in the environment, the direction and magnitude of user inputs, and the cost function used by the implementation of the hindsight optimization algorithm.*

5 COMPARING ALGORITHMS

Given the effectiveness of quality diversity in automatically generating a diverse range of test scenarios, we propose it as a method to contrast the performance of different algorithms. We continue using the shared autonomy domain as example, and we compare hindsight optimization [36] against policy blending [16].

Policy Blending. In shared autonomy, policy blending is a widely used alternative to POMDP-based methods in shared autonomy, since it provides an intuitive interface for combining robotic assistance with user inputs [11, 16, 24, 33, 45, 52]. In this approach, the robot’s and user’s actions are treated as two independent sources. The final robot motion is determined by an arbitration function that regulates the two inputs, based on the robot’s confidence about the user’s goal. A special case of policy blending is *linear blending*. Theoretical analysis of linear blending [65] has shown that it can lead to unsafe behavior in the presence of obstacles.

We want to empirically confirm these theoretical findings and assess how hindsight optimization and linear policy blending perform in the presence of obstacles. We thus created a new environment with one goal object and a second object that acts as an obstacle. Since there is only one unique goal object, there will be no failure cases arising from incorrect inference as in Sec. 4.

In linear blending, robot and human inputs are weighted by the arbitration coefficients α and $1 - \alpha$ respectively. Previous work [16] considers two types: an “aggressive” blending, where the robot takes over ($\alpha = 1.0$) if confidence is above a threshold ($conf \geq 0.4$), and a “timid” blending where α linearly increases from 0 to 0.6 for $0.4 \leq conf \leq 0.8$. When we have only one goal, confidence is

always 1.0 and “aggressive” blending and hindsight optimization are identical. Therefore, we consider only the “timid” mode which sets α to 0.6.

Obstacle Modeling. While the hindsight optimization implementation [42] models the user as minimizing the Euclidean distance between the robot’s end-effector and their goal, this is no longer applicable in the presence of obstacles, since a direct path to the goal may collide with the obstacle. Exact computation of the value function is also infeasible, given that the state and action spaces are continuous and the robot acts in real-time. We simplify the computation by modeling the obstacle as a sphere and, if a direct path to the goal intersects with the sphere, we find the intersecting points and approximate the value function as the length of the shortest path to the goal that wraps around the sphere. We do the same for the human waypoints (before adding any disturbances), so that an optimal human will follow the shortest collision-free path to the goal. For robustness, if the end-effector touches the surface of the sphere, it receives an additional velocity command in the direction away from the center of the sphere, similarly to a potential field [12]. We found the sphere approximation simplification adequate for detecting collisions with the hindsight optimization and policy blending algorithms.

Experiment. We fix the position of the goal object and the obstacle in the y-axis, so that the obstacle o is always between the robot and the goal, and we search for the coordinates ($\phi = (g_x, o_x)$) in the x-axis (Fig. 6). The goal object has three target grasp poses. Identically to Sec. 4, we search for the disturbances to the human inputs ($\theta = (d_1, \dots, d_5)$). We specify three BCs: the distance between the two objects in the x-axis, the human variation – identically to Sec. 4 – and a binary BC, $BC_{collision} \in \{True, False\}$ indicating whether the robot’s end-effector has collided with the obstacle. As before, we set the assessment function f to the time to completion, with a maximum limit of 15s. The task terminates if the robot reaches the goal or if it collides with the obstacle. We generate 20,000 scenarios with one run of MAP-Elites to test the two algorithms.

Analysis. Fig. 5 shows the archives generated for the policy blending and the hindsight optimization algorithms. For each algorithm, we present two 2D archives, one with $BC_{collision} = True$ and one with $BC_{collision} = False$. We compare the archives of the two algorithms in terms of coverage and quality of the scenarios.

Coverage. The coverage was 47% for hindsight optimization, compared to 69% for policy blending. We observe that the archive with $BC_{collision} = True$ is heavily populated in policy blending (Fig. 5a). The archive shows collisions even for a nearly optimal human; while both the human and robot inputs were collision free, sometimes they pointed towards opposite sides of the obstacle, and blending the two resulted in collision (Fig. 6(left)). This result matches the theoretical predictions [65] of unsafe trajectories in linear blending.

The $BC_{collision} = True$ archive in Fig. 5a also shows that when the horizontal distance exceeds a threshold, the robot can reach the goal with a nearly straight path, and collision occurs only when the human inputs are very noisy (Fig. 6(right)).

On the other hand, hindsight optimization resulted in a nearly empty archive when $BC_{collision} = True$. The reason is that it uses the human inputs as observations, and the robot’s motion is determined only by the robot’s policy; the few sparse collisions are

¹<https://youtu.be/2-JCO3dUHsA>

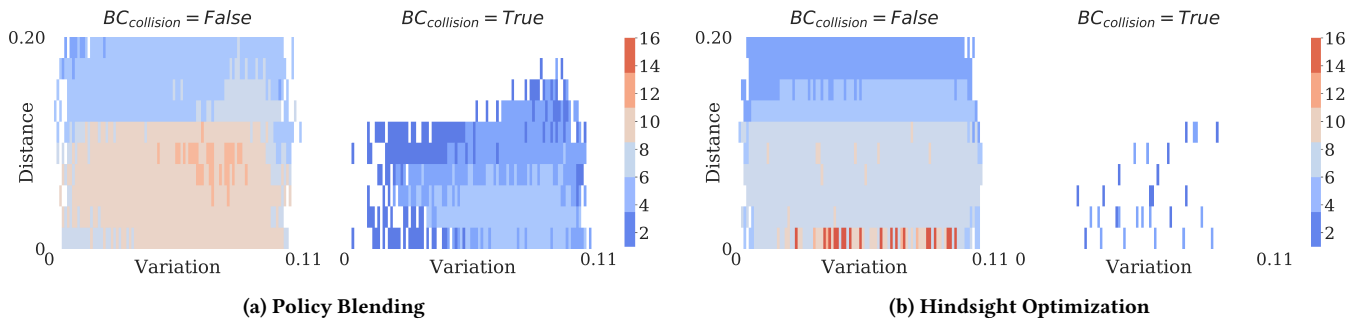


Figure 5: Archives generated with MAP-Elites for the policy blending and hindsight optimization algorithms. The colors of the cells in the archives represent time to task completion in seconds.

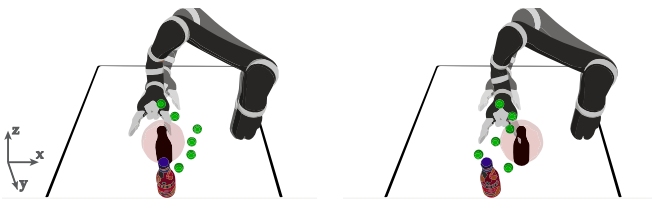


Figure 6: Scenarios where the policy blending algorithm results in collision with an obstacle, approximated by a sphere. (Left) While the human and robot trajectories are each collision-free, blending the two results to collision when they point towards opposite sides of the obstacle. (Right) Blending with a very noisy human input results in collision.

artifacts of the OpenRAVE environment, occurring because of infrequent lags in sending velocity commands to the robot.

Scenario Assessment. When $BC_{collision} = False$, the average time to completion was 7.95s for policy blending and 6.70s for hindsight optimization, indicating that policy blending took more time to finish the task. This result matches previous human subjects experiments [35], where policy blending took longer than hindsight optimization, and it was caused by two factors: (1) Often the human and robot inputs would point to opposite directions, resulting in velocities of small magnitudes when blended together. (2) The human inputs were proportional to the distance to the next waypoint, spiking at the waypoints and decreasing until the next waypoint (Sec. 4.2). This resulted in parts of the trajectory where the human inputs were of smaller magnitude than the robot’s, so blending the two gave smaller velocity commands than treating the human inputs as observations. The red bars in hindsight optimization (Fig. 5b) indicate timeouts; when the goal object was exactly behind the obstacle, the robot sometimes oscillated between taking a grasping position and moving away from the sphere.

6 Discussion

Experimental Findings. We found that failure scenarios for hindsight optimization occur when the two goals are close to each other and the human inputs are noisy, or when one goal is in front of the other. In the latter case, failure occurs even if the human input is

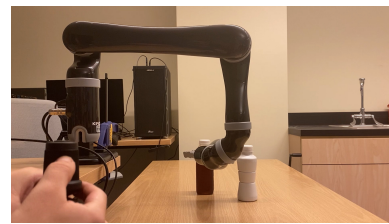


Figure 7: The supplemental video shows the generated scenarios in the real world with actual joystick inputs.

nearly optimal in minimizing the distance to the desired goal. In both cases, the robot becomes over-confident about the wrong goal and gets “stuck” there.

An important factor is the linear decrease of the cost in the vicinity of the goal objects. When specifying the cost function, it would be prudent to make the distance threshold for the linear decrease proportional to the distance between the goal objects, rather than setting it to an absolute value.

Other potential measures to avoid the system’s overconfidence towards the wrong goal are: (1) including the Shannon entropy with respect to all the goals in the cost function [37] to penalize actions that result in very high confidence to one specific goal; (2) assigning a non-zero probability that the user changes their mind throughout the task and switches goals [32, 54]. It would be interesting to investigate the effect of more “conservative” assistance on subjective and objective metrics of the robot’s performance.

Finally, while linear policy blending naturally gives more control to the user and it is preferred by users in simple tasks [35], we empirically verified that it can generate unsafe trajectories, even if the individual human and robot inputs are safe.

To show that the presented scenarios can occur in deployed systems, in the supplemental video we reproduce them in the real world with actual inputs through a joystick interface (Fig. 7).

Limitations. An important challenge is how to effectively characterize the behavior spaces. While we have assumed bounded behavior spaces, the rationality coefficient does not meet this assumption, which resulted in elites accumulating in the upper bound of the rationality in the archive (Fig. 2). Adapting the boundaries

of the space dynamically based on the distribution of generated scenarios [19] could improve coverage in this case.

We focused on how to effectively search the generative space of scenarios, but not on the scenario generation methods themselves. Realism is an important future consideration; although we generate human actions with certain rationality measures, there is no guarantee that real users would behave in a similar manner. In human training, realism can be measured through a modified Turing test designed to require humans to distinguish generated scenarios from human authored ones [48]. Alternatively, we could do a user study where we place objects in the same locations as our failure scenarios and observe whether participants perform similar actions that cause failures.

Implications. Finding failure scenarios of HRI algorithms will play a critical role in the adoption of these systems. Using the shared autonomy as example domain, we proposed quality diversity as an approach for automatically generating scenarios that assess the performance of HRI algorithms and illustrated a path for future work. We are excited about applications of quality diversity algorithms as test oracles in verification systems [41], as well as in other HRI domains; we are confident that highlighting previously unknown strengths and weaknesses of HRI algorithms will bring about a new understanding of the state-of-the-art in computational HRI and open up new research challenges and opportunities.

References

- [1] Daniel Aarno, Staffan Ekvall, and Danica Kragic. 2005. Adaptive virtual fixtures for machine-assisted teleoperation tasks. In *Robotics and Automation, 2005. ICRA 2005. Proceedings of the 2005 IEEE International Conference on*. IEEE, 1139–1144.
- [2] Y. Abeyirigoonawardena, F. Shkurti, and G. Dudek. 2019. Generating Adversarial Driving Scenarios in High-Fidelity Simulators. In *2019 International Conference on Robotics and Automation (ICRA)*. 8271–8277. <https://doi.org/10.1109/ICRA.2019.8793740>
- [3] Dejanira Araiza-Illan, Anthony G Pipe, and Kerstin Eder. 2016. Intelligent agent-based stimulation for testing robotic software in human-robot interactions. In *Proceedings of the 3rd Workshop on Model-Driven Robot Software Engineering*. 9–16.
- [4] Dejanira Araiza-Illan, David Western, Anthony Pipe, and Kerstin Eder. 2015. Coverage-Driven Verification—. In *Haifa Verification Conference*. Springer, 69–84.
- [5] Dejanira Araiza-Illan, David Western, Anthony G Pipe, and Kerstin Eder. 2016. Systematic and realistic testing in simulation of control code for robots in collaborative human-robot interactions. In *Annual Conference Towards Autonomous Robotic Systems*. Springer, 20–32.
- [6] James Arnold and Rob Alexander. 2013. Testing Autonomous Robot Control Software Using Procedural Content Generation. In *Proceedings of the 32Nd International Conference on Computer Safety, Reliability, and Security - Volume 8153 (SAFECOMP 2013)*. Springer-Verlag New York, Inc., New York, NY, USA, 33–44. https://doi.org/10.1007/978-3-642-40793-2_4
- [7] Anne Auger and Nikolaus Hansen. 2005. A restart CMA evolution strategy with increasing population size. In *2005 IEEE congress on evolutionary computation*, Vol. 2. IEEE, 1769–1776.
- [8] Chris L Baker, Joshua B Tenenbaum, and Rebecca R Saxe. 2007. Goal inference as inverse planning. In *Proceedings of the Annual Meeting of the Cognitive Science Society*, Vol. 29.
- [9] Rafał Biedrzycki. 2020. Handling bound constraints in CMA-ES: An experimental study. *Swarm and Evolutionary Computation* 52 (2020), 100627.
- [10] Zeungnam Bien, Myung-Jin Chung, Pyung-Hun Chang, Dong-Soo Kwon, Dae-Jin Kim, Jeong-Su Han, Jae-Hean Kim, Do-Hyung Kim, Hyung-Soon Park, Sang-Hoon Kang, et al. 2004. Integration of a rehabilitation robotic system (KARES II) with human-friendly man-machine interaction units. *Autonomous robots* 16, 2 (2004), 165–191.
- [11] Tom Carlson and Yiannis Demiris. 2012. Collaborative control for a robotic wheelchair: evaluation of performance, attention, and workload. *IEEE Transactions on Systems, Man, and Cybernetics, Part B (Cybernetics)* 42, 3 (2012), 876–888.
- [12] Jacob W Crandall and Michael A Goodrich. 2002. Characterizing efficiency of human robot interaction: A case study of shared-control teleoperation. In *IEEE/RSJ international conference on intelligent robots and systems*, Vol. 2. IEEE, 1290–1295.
- [13] Antoine Cully, Jeff Clune, Danesh Tarapore, and Jean-Baptiste Mouret. 2015. Robots that can adapt like animals. *Nature* 521, 7553 (2015), 503.
- [14] Rosen Diankov and James Kuffner. 2008. Openrave: A planning architecture for autonomous robotics. *Robotics Institute, Pittsburgh, PA, Tech. Rep. CMU-RI-TR-08-34 79* (2008).
- [15] Finale Doshi and Nicholas Roy. 2007. Efficient model learning for dialog management. In *Proceedings of the ACM/IEEE international conference on Human-robot interaction*. ACM, 65–72.
- [16] A.D. Dragan and S.S. Srinivasa. 2012. Formalizing Assistive Teleoperation. In *Proc. Robotics: Science and Systems Conference*.
- [17] Andrew H Fagg, Michael Rosenstein, Robert Platt, and Roderic A Grupen. 2004. Extracting user intent in mixed initiative teleoperator control. In *Proceedings of the American Institute of Aeronautics and Astronautics Intelligent Systems Technical Conference*.
- [18] Jaime F Fisac, Andrea Bajcsy, Sylvia L Herbert, David Fridovich-Keil, Steven Wang, Claire J Tomlin, and Anca D Dragan. 2018. Probabilistically safe robot planning with confidence-based human predictions. *arXiv preprint arXiv:1806.00109* (2018).
- [19] Matthew C. Fontaine, Scott Lee, L. B. Soros, Fernando de Mesentier Silva, Julian Togelius, and Amy K. Hoover. 2019. Mapping Hearthstone Deck Spaces through MAP-Elites with Sliding Boundaries. In *Proceedings of the Genetic and Evolutionary Computation Conference (GECCO '19)*. ACM, New York, NY, USA, 161–169. <https://doi.org/10.1145/3321707.3321794>
- [20] Matthew C Fontaine, Ruilin Liu, Julian Togelius, Amy K Hoover, and Stefanos Nikolaidis. 2020. Illuminating Mario Scenes in the Latent Space of a Generative Adversarial Network. *arXiv preprint arXiv:2007.05674* (2020).
- [21] Matthew C Fontaine, Julian Togelius, Stefanos Nikolaidis, and Amy K Hoover. 2020. Covariance Matrix Adaptation for the Rapid Illumination of Behavior Space. *Proceedings of the Genetic and Evolutionary Computation Conference* (2020).
- [22] Alessio Gambi, Marc Mueller, and Gordon Fraser. 2019. Automatically Testing Self-driving Cars with Search-based Procedural Content Generation. In *Proceedings of the 28th ACM SIGSOFT International Symposium on Software Testing and Analysis (ISSTA 2019)*. ACM, New York, NY, USA, 318–328. <https://doi.org/10.1145/3293882.3330566>
- [23] Jeremy H Gillula, Gabriel M Hoffmann, Haomiao Huang, Michael P Vitus, and Claire J Tomlin. 2011. Applications of hybrid reachability analysis to robotic aerial vehicles. *The International Journal of Robotics Research* 30, 3 (2011), 335–354.
- [24] Deepak Gopinath, Siddharth Jain, and Brenna D Argall. 2016. Human-in-the-loop optimization of shared autonomy in assistive robotics. *IEEE Robotics and Automation Letters* 2, 1 (2016), 247–254.
- [25] Daniele Gravina, Ahmed Khalifa, Antonios Liapis, Julian Togelius, and Georgios N Yannakakis. 2019. Procedural content generation through quality diversity. In *2019 IEEE Conference on Games (CoG)*. IEEE, 1–8.
- [26] Nikolaus Hansen. 2009. Benchmarking a BI-population CMA-ES on the BBOB-2009 function testbed. In *Proceedings of the 11th Annual Conference Companion on Genetic and Evolutionary Computation Conference: Late Breaking Papers*. 2389–2396.
- [27] Nikolaus Hansen. 2016. The CMA evolution strategy: A tutorial. *arXiv preprint arXiv:1604.00772* (2016).
- [28] Kris Hauser. 2013. Recognition, prediction, and planning for assisted teleoperation of freeform tasks. *Autonomous Robots* 35, 4 (2013), 241–254.
- [29] Mark Hendriks, Sebastiaan Meijer, Joeri Van Der Velden, and Alexandru Iosup. 2013. Procedural content generation for games: A survey. *ACM Transactions on Multimedia Computing, Communications, and Applications (TOMM)* 9, 1 (2013), 1–22.
- [30] Laura V Herlant, Rachel M Holladay, and Siddhartha S Srinivasa. 2016. Assistive teleoperation of robot arms via automatic time-optimal mode switching. In *The Eleventh ACM/IEEE International Conference on Human Robot Interaction*. IEEE Press, 35–42.
- [31] Ronald C Hofer, Edward Ramirez, and Scott H Smith. 1998. (1998).
- [32] Siddharth Jain and Brenna Argall. 2018. Recursive Bayesian human intent recognition in shared-control robotics. In *2018 IEEE/RSJ International Conference on Intelligent Robots and Systems (IROS)*. IEEE, 3905–3912.
- [33] Siddharth Jain and Brenna Argall. 2019. Probabilistic human intent recognition for shared autonomy in assistive robotics. *ACM Transactions on Human-Robot Interaction (THRI)* 9, 1 (2019), 1–23.
- [34] Siddharth Jain, Ali Farshchiansadegh, Alexander Broad, Farnaz Abdollahi, Ferdinando Mussa-Ivaldi, and Brenna Argall. 2015. Assistive robotic manipulation through shared autonomy and a body-machine interface. In *2015 IEEE international conference on rehabilitation robotics (ICORR)*. IEEE, 526–531.
- [35] Shervin Javdani, Henny Admoni, Stefania Pellegrinelli, Siddhartha S Srinivasa, and J Andrew Bagnell. 2018. Shared autonomy via hindsight optimization for teleoperation and teaming. *The International Journal of Robotics Research* (2018), 0278364918776060.
- [36] S. Javdani, S. S. Srinivasa, and J.A. Bagnell. 2015. Shared Autonomy via Hindsight Optimization. In *Proc. Robotics: Science and Systems Conference*.
- [37] Hong Jun Jeon, Dylan P Losey, and Dorsa Sadigh. 2020. Shared Autonomy with Learned Latent Actions. *arXiv preprint arXiv:2005.03210* (2020).

- [38] Ahmed Khalifa, Michael Cerny Green, Gabriella Barros, and Julian Togelius. 2019. Intentional computational level design. In *Proceedings of The Genetic and Evolutionary Computation Conference*. 796–803.
- [39] Jonathan Kofman, Xianghai Wu, Timothy J Luu, and Siddharth Verma. 2005. Teleoperation of a robot manipulator using a vision-based human-robot interface. *IEEE Transactions on Industrial Electronics* 52, 5 (2005), 1206–1219.
- [40] Hema S Koppula and Ashutosh Saxena. 2016. Anticipating human activities using object affordances for reactive robotic response. *IEEE Transactions on Pattern Analysis and Machine Intelligence* 38, 1 (2016), 14–29.
- [41] Hadas Kress-Gazit, Kerstin Eder, Guy Hoffman, Henny Admoni, Brenna Argall, Ruediger Ehlers, Christoffer Heckman, Nils Jansen, Ross Knepper, Jan Křetínský, et al. 2020. Formalizing and Guaranteeing* Human-Robot Interaction. *arXiv preprint arXiv:2006.16732* (2020).
- [42] Personal Robotics Lab. 2017. https://github.com/personalrobotics/ada_assistance_policy/.
- [43] Thanh Mung Lam, Harmen Wigert Boschloo, Max Mulder, and Marinus M Van Paassen. 2009. Artificial force field for haptic feedback in UAV teleoperation. *IEEE Transactions on Systems, Man, and Cybernetics-Part A: Systems and Humans* 39, 6 (2009), 1316–1330.
- [44] Ming Li and Allison M Okamura. 2003. Recognition of operator motions for real-time assistance using virtual fixtures. In *Haptic Interfaces for Virtual Environment and Teleoperator Systems, 2003. HAPTICS 2003. Proceedings. 11th Symposium on*. IEEE, 125–131.
- [45] Qinan Li, Weidong Chen, and Jingchuan Wang. 2011. Dynamic shared control for human-wheelchair cooperation. In *2011 IEEE International Conference on Robotics and Automation*. IEEE, 4278–4283.
- [46] Michael L Littman, Anthony R Cassandra, and Leslie Pack Kaelbling. 1995. Learning policies for partially observable environments: Scaling up. In *Machine Learning Proceedings 1995*. Elsevier, 362–370.
- [47] Dylan P Losey, Krishnan Srinivasan, Ajay Mandelkar, Animesh Garg, and Dorsa Sadigh. 2019. Controlling assistive robots with learned latent actions. *arXiv preprint arXiv:1909.09674* (2019).
- [48] Glenn A. Martin. 2012. *Automatic Scenario Generation using Procedural Modeling Techniques*. Ph.D. Dissertation. University of Central Florida.
- [49] Glenn A. Martin, Charles E. Hughes, Sae Schatz, and Denise Nicholson. 2010. The Use of Functional L-systems for Scenario Generation in Serious Games. In *Proceedings of the 2010 Workshop on Procedural Content Generation in Games (PCGames '10)*. ACM, New York, NY, USA, Article 6, 5 pages. <https://doi.org/10.1145/1814256.1814262>
- [50] Douglas Morrison, Peter Corke, and Jurgen Leitner. 2020. EGAD! an Evolved Grasping Analysis Dataset for diversity and reproducibility in robotic manipulation. *IEEE Robotics and Automation Letters* (2020).
- [51] Jean-Baptiste Mouret and Jeff Clune. 2015. Illuminating search spaces by mapping elites. *arXiv preprint arXiv:1504.04909* (2015).
- [52] Katharina Muelling, Arun Venkatraman, Jean-Sebastien Valois, John E. Downey, Jeffrey Weiss, Shervin Javdani, Martial Hebert, Andrew B. Schwartz, Jennifer L. Collinger, and J. Andrew Bagnell. 2017. Autonomy Infused Teleoperation with Application to Brain Computer Interface Controlled Manipulation. *Auton. Robots* 41, 6 (Aug. 2017), 1401–1422.
- [53] Galen E. Mullins, Paul G. Stankiewicz, R. Chad Hawthorne, and Satyandra K. Gupta. 2018. Adaptive generation of challenging scenarios for testing and evaluation of autonomous vehicles. *Journal of Systems and Software* 137 (2018), 197 – 215. <https://doi.org/10.1016/j.jss.2017.10.031>
- [54] Stefanos Nikolaidis, David Hsu, and Siddhartha Srinivasa. 2017. Human-robot mutual adaptation in collaborative tasks: Models and experiments. *The International Journal of Robotics Research* 36, 5-7 (2017), 618–634.
- [55] S. Nikolaidis, Zhu. Y., D. Hsu, and S.S. Srinivasa. 2017. Human-Robot Mutual Adaptation in Shared Autonomy. In *Proc. Human Robot Interaction Conference*.
- [56] Justin K. Pugh, Lisa B. Soros, and Kenneth O. Stanley. 2016. Quality Diversity: A New Frontier for Evolutionary Computation. *Frontiers in Robotics and AI* 3 (2016), 40. <https://doi.org/10.3389/frobt.2016.00040>
- [57] Justin K Pugh, Lisa B Soros, Paul A Szerlip, and Kenneth O Stanley. 2015. Confronting the challenge of quality diversity. In *Proceedings of the 2015 Annual Conference on Genetic and Evolutionary Computation*. 967–974.
- [58] Siddharth Reddy, Sergey Levine, and Anca Dragan. 2018. Shared Autonomy via Deep Reinforcement Learning. *arXiv preprint arXiv:1802.01744* (2018).
- [59] Jing Ren, Rajni V Patel, Kenneth A McIsaac, Gerard Guiraudon, and Terry M Peters. 2008. Dynamic 3-D virtual fixtures for minimally invasive beating heart procedures. *IEEE transactions on medical imaging* 27, 8 (2008), 1061–1070.
- [60] E. Rocklage, H. Kraft, A. Karatas, and J. Seewig. 2017. Automated scenario generation for regression testing of autonomous vehicles. In *2017 IEEE 20th International Conference on Intelligent Transportation Systems (ITSC)*. 476–483. <https://doi.org/10.1109/ITSC.2017.8317919>
- [61] Noor Shaker, Julian Togelius, and Mark J. Nelson. 2016. *Procedural Content Generation in Games: A Textbook and an Overview of Current Research*. Springer.
- [62] Davy Smith, Laurissa Tokarchuk, and Geraint Wiggins. 2016. Rapid phenotypic landscape exploration through hierarchical spatial partitioning. In *International conference on parallel problem solving from nature*. Springer, 911–920.
- [63] Aaron Steinfeld, Odest Chadwicke Jenkins, and Brian Scassellati. 2009. The oz of wizard: simulating the human for interaction research. In *Proceedings of the 4th ACM/IEEE international conference on Human robot interaction*. 101–108.
- [64] Andrea Thomaz, Guy Hoffman, and Maya Cakmak. 2016. Computational human-robot interaction. *Foundations and Trends in Robotics* 4, 2-3 (2016), 105–223.
- [65] Pete Trautman. 2015. Assistive planning in complex, dynamic environments: a probabilistic approach. In *2015 IEEE International Conference on Systems, Man, and Cybernetics*. IEEE, 3072–3078.
- [66] Vassilis Vassiliades and Jean-Baptiste Mouret. 2018. Discovering the Elite Hyper-volume by Leveraging Interspecies Correlation. In *Proceedings of the Genetic and Evolutionary Computation Conference*. 149–156.
- [67] Eduardo Veras, Karan Khokar, Redwan Alqasemi, and Rajiv Dubey. 2009. Scaled telerobotic control of a manipulator in real time with laser assistance for ADL tasks. In *Mechatronics and its Applications, 2009. ISMA'09. 6th International Symposium on*. IEEE, 1–6.
- [68] Roman Vershynin. 2018. *Random Vectors in High Dimensions, page 3869*. Cambridge University Press.
- [69] Zhikun Wang, Katharina Mülling, Marc Peter Deisenroth, Heni Ben Amor, David Vogt, Bernhard Schölkopf, and Jan Peters. 2013. Probabilistic movement modeling for intention inference in human-robot interaction. *The International Journal of Robotics Research* 32, 7 (2013), 841–858.
- [70] Brian D Ziebart, Andrew L Maas, J Andrew Bagnell, and Anind K Dey. 2008. Maximum Entropy Inverse Reinforcement Learning. In *Proc. AAAI Conference on Artificial Intelligence*. 1433–1438.
- [71] Alexander Zook, Stephen Lee-Urban, Mark O Riedl, Heather K Holden, Robert A Sottilare, and Keith W Brawner. 2012. Automated scenario generation: toward tailored and optimized military training in virtual environments. In *Proceedings of the international conference on the foundations of digital games*. 164–171.